ELSEVIER

Chemical Engineering Journal 137 (2008) 54–61

Chemical Engineering Journal

www.elsevier.com/locate/cej

Synthesis and characterization of MCM-41 spheres inside bioactive glass–ceramic scaffold

R. Mortera [a,b], B. Onida [a,b], S. Fiorilli [a,c], V. Cauda [a,b], C. Vitale Brovarone [a,b], F. Baino [a,b], E. Vernè [a,b], E. Garrone [a,b,*]

[a] *Dipartimento di Scienza dei Materiali e Ingegneria Chimica, Politecnico di Torino, Corso Duca degli Abruzzi, 24-10125 Torino, Italy*

[b] *INSTM, Torino Politecnico Unit, Torino, Italy*

[c] *LaTEMAR, Centre of Excellence, Torino, Italy*

Received 30 May 2007; received in revised form 24 July 2007; accepted 31 July 2007

Abstract

Composite systems have been prepared, combining the drug up-take and release properties of MCM-41 silica sub-micron spheres with those of a bioactive glass–ceramic macroporous scaffold belonging to the SiO_2–CaO–K_2O (SCK) system (potentially able to promote successful osteointegration in tissue engineering).

The systems are prepared by dipping the glass–ceramic scaffold into the MCM-41 synthesis solution. To this purpose, the pH of the MCM-41 synthesis solution has been lowered with respect to the usual literature procedure to minimize the detrimental effects of the impregnation treatment on glass–ceramic scaffolds that were observed in a previous work by the author.

MCM-41–SCK composite scaffolds have been characterized by means of XRD, N_2 adsorption, thermogravimetry and Scanning Electron Microscopy (coupled with EDS analysis).

The adsorption capacity toward ibuprofen, tested as model drug, is three times higher than that of the MCM-41-free scaffold, because of the presence of the ordered mesoporous silica. Also the release behaviour in SBF at 37 °C is strongly affected by the presence of MCM-41 inside the scaffold macropores.

Keywords: MCM-41; Drug release; Bioactive glass–ceramic; Composite scaffold for tissue engineering

1. Introduction

One of the most interesting fields of research in the orthopaedic surgery and in tissue engineering concerns the use of porous materials to reproduce the complex morphology of bone tissues [1,2]. Such materials, inserted on damaged bones should restore bone loss caused from surgery and pathological affections. Among artificial grafts (scaffolds), hydroxyapatite, β-tricalcium phosphate and more recently bioactive glasses have been widely studied in the last years for guided bone regeneration. In order to be used as bone grafts, the scaffolds should possess a porous structure characterized by open macropores of a few 100 μm highly interconnected and sufficient mechanical strength (higher than 1–2 MPa) [3–7]. Compared to crystalline ceramics, bioactive glasses possess unique properties due to their ability in stimulating the bone regeneration process through a complex mechanism of ions exchange that lead to the precipitation on their surfaces of a microcrystalline hydroxyapatite which favours a strong chemical bond with the surrounding bone tissues. This unique feature is known as bioactivity and was described by L. Hench in 1970 [8]. Besides, as far as the scaffolds production is concerned, glasses are generally more versatile than crystalline ceramics due to their ability of gradually soften with increasing temperatures.

The first problem occurring after an implant is the great exposure to inflammatory risks with further complications, e.g. septicaemia and loss of mobility of the dealt zone [9,10]. To avoid these disadvantages, large amount of anti-inflammatory and antibiotics are administered to the patient, with a remarkable

* Corresponding author at: INSTM, Torino Politecnico Unit, 10125 Torino, Italy. Tel.: +39 0115644661; fax: +39 011 5644699.

E-mail address: edoardo.garrone@polito.it (E. Garrone).

1385-8947/$ – see front matter © 2007 Elsevier B.V. All rights reserved.
doi:10.1016/j.cej.2007.07.094

lengthening of the stays in hospital and the times of recovery.

For this reasons, the interest in devices able to release in a controlled way molecules of specific drugs, hormones and growth factors has increased considerably during the last few years. Many polymer-based pharmaceutical carrier systems have been developed as first means of controlling temporal drug delivery [11]. To combine bone-generating ability (bioactivity and porous structure) with controlled release properties, other sol–gel derived silica-based materials have been investigated [12–14]. These kinds of materials, however, present a heterogeneous pore size distribution, which inhibits the real possibility of delivery control.

Vallet-Regí et al. extended the release studies to ordered mesoporous silicas [15] which, at variance with most organic polymer-derived matrices, exhibit a narrow pore size distribution in combination with a high specific surface area [16]. These features, combined with the possibility to modulate pore diameter in a wide range by varying synthesis conditions, favour the incorporation of drug into the structures and, above all, allow a controlled release. Several studies have been carried out and many mesoporous silicas have been suggested as matrices for drug delivery systems, especially for non-steroidal anti-inflammatory drugs [17–19].

Tourné-Peteilh et al. proposed the functionalization of the hexagonal mesophase MCM-41 with 3-glycidoxypropylsilane in order to obtain a covalent bond between the drug and the silica walls [20].

As far as the health effects of silica are concerned, precipitated amorphous silicas have always been considered as non-toxic [21]. For this reason it is conceivable to combine them with bioactive materials used for bone implants.

In a previous work [22], SBA-15 mesoporous silica has been incorporated inside a bioactive glass–ceramics scaffold belonging to the SiO_2–CaO–K_2O (SCK) system [23], to obtain a multifunctional system potentially able to promote successful integration of implanted prosthesis, and to deliver locally species of pharmaceutical interest.

Starting from the same SCK scaffold, in the present contribution the study is extended to MCM-41 silica. On the one hand, a mesoporous silica with narrower pore size and greater specific surface area with respect to SBA-15 may be desirable when the small drug molecules are considered. On the other hand, it is interesting to explore the effect of basic synthesis conditions, at variance with strongly acidic, on the properties of the final system. Bioactive glass–ceramics scaffold, in fact, are not inert to the chemical treatment necessary for the precipitation of mesoporous silica, and both the morphology and the mechanical properties might be affected [24].

MCM-41–SCK composite scaffolds have been prepared and characterized by means of X-ray diffraction, N_2 adsorption/desorption isotherms, differential thermogravimetry (DTG), scanning electron microscopy (SEM) coupled with EDS analysis.

Ibuprofen, extensively adopted in the literature [15,17–20], has been chosen as model drug to characterize up-take capacity and release properties.

2. Experimental

2.1. Synthesis of MCM-41 at mildly basic pH

The procedure adopted to prepare MCM-41 was that reported by Grün et al. [25], which yields sub-micron sized spherical particles, i.e. a morphology desirable for drug delivery. The pH of the synthesis batch is strongly basic due to the presence of ammonia (pH around 11). The procedure has been modified in order to lower the pH, so to have a less aggressive medium for the SCK scaffold impregnation aiming to avoid damages of the scaffold.

Four samples of MCM-41 (herein named MCM-41-*n*, with *n* referring to the synthesis pH) were prepared, starting from the procedure reported by Grün et al. [25] (MCM-41-10.8) and lowering the ammonia concentration of the synthesis solution (MCM-41-10.5, MCM-41-9.5, MCM-41-9.0).

The same quantity of *n*-hexadecyltrimethylammonium bromide (C_{16}TMABr, Aldrich) was dissolved into different basic solutions with variable concentration of aqueous ammonia (33 wt.%, Riedel-de Häen), followed by the addition of tetraethylorthosilicate (TEOS 98%, Aldrich). The reactant molar ratio was: 1 TEOS:0.3 C_{16}TMABr:*x* NH_3:144 H_2O:58 EtOH, with *x* ranging from 11 to 0.129 and pH accordingly ranging from 10.8 to 9.0.

After stirring for 2 h at room temperature, the products were filtered, dried overnight at 90 °C and calcined at 450 °C for 7 h in flowing dry air (heating rate: 1 °C/min).

2.2. Preparation of SCK scaffold

A bioactive glass belonging to the SiO_2–CaO–K_2O presenting the following molar percentage composition: 50% SiO_2–44% CaO–6% K_2O was prepared by melting in a platinum crucible at 1500 °C for 1 h. The molten glass was quenched in water to obtain a frit that was grounded by ball milling and sieved below 106 μm. SCK powders were then mixed with polyethylene particles having a grain size within 300 μm and 600 μm using a 1:1 volume rate. 8 g of mixed powders were then uniaxially pressed for 10 s at 150 MPa using few drops of propanol as liquid binder in order to produce a defects-free compact of powders (green) shaped as a disk. Green compacts were thermally treated 950 °C for 2 h in air to induce the sintering process of SCK powders and the burning-out of the organic phase. The material obtained from the thermal treatment is a macroporous glass–ceramic scaffold characterized by interconnected macropores in the range 200–600 μm, micropores of 1–10 μm and a total porosity over 60 vol.% [23].

2.3. Preparation of MCM-41–SCK composites scaffolds

The procedure for the preparation of MCM-41–SCK composite scaffolds consisted in four steps, i.e. *hydrolysis* of TEOS in MCM-41-synthesis solution, *dipping* of a SCK scaffold for impregnation, *drying* of the impregnated SCK scaffold and *calcination*.

The synthesis batch characterized by pH 9.0 was used to impregnate the SCK scaffold due to its less severe synthesis conditions.

After TEOS addition, the solution has been stirred for 10 min to promote the hydrolysis of the silica precursor (*hydrolysis step*).

Two SCK scaffolds having a volume of about 0.55 cm^3 and a mass of about 0.9 g have been soaked in the silica synthesis batch for 11 min, under continuous stirring (*dipping step*).

The overall duration of both hydrolysis and dipping steps does not exceed 21 min, the time after which precipitation of the MCM-41 mesophase in the synthesis batch is observed.

Another SCK scaffold, used as reference (herein denoted has SCK-ref), has been soaked for the same time in the synthesis solution without TEOS.

After separation from the solution, the two MCM-41-impregnated SCK scaffolds were treated following two different procedures (*drying step*): one was dried in a covered vessel at 90 °C overnight (hereafter named MCM-41–SCK-1), whereas the other was maintained for 2 h at room temperature in a covered vessel and then treated at 90 °C overnight (hereafter denoted as MCM-41–SCK-2). This latter treatment resembles more closely the synthesis of MCM-41 in powder form, where the synthesis batch is stirred for 2 h at room temperature after the appearance of the precipitate.

SCK-ref was dried following the same procedure as MCM-41–SCK-1 composite scaffold.

All samples were calcined at 200 °C in nitrogen for 1 h and then at 450 °C in air for 7 h (heating rate: 1 °C/min).

2.4. Characterization

The systems have been characterized by means of powder X-ray diffraction (X'Pert Philips, Cu Kα radiation), nitrogen adsorption measurements at 77 K (Quantachrome Autosorb1), Field Emission Scanning Electron Microscopy (Assing FESEM Supra 25) associated with Energy Dispersive Spectroscopy (EDS, Oxford Instrument INCA X-Sight) and thermogravimetry (Mettler Toledo, TGA/SDTA 851°).

For XRD and thermogravimetry measurements samples have been ground to powder.

BET specific surface areas have been calculated in the relative pressure range 0.04–0.1 and pore size has been evaluated following the BJH method [26].

2.5. Drug up-take

Adsorption of ibuprofen (99.9%, Sigma) has been carried out putting in contact a solution of ibuprofen in pentane (33 mg/ml) with the sample for 3 days at room temperature. The pentane was used to substitute the commonly used but toxic hexane [27,28]. We tried various solvents (pentane, diethylether, ethanol and cyclohexane) as an alternative to hexane, among which pentane shows highest up-take values, which are also very close to those observed for hexane, allowing a reasonable comparison with literature data.

A Cary 500 Scan UV–vis spectrophotometer was used to evaluate the amount of ibuprofen absorbed by the samples, calculated from the difference in the concentration of ibuprofen in solution before and after contact with the sample, on the basis of the absorption at 263 nm, typical of the molecule. The calibration curve has been calculated using pentane solutions of ibuprofen in the same concentration range.

2.6. Drug release

Drug delivery evaluation *in vitro* has been performed by soaking the samples in 30 ml of stirred simulate body fluid (SBF) solution [29], maintained at 37 °C. The amount of released ibuprofen has been evaluated in aliquots of the solution (1.5 ml), measuring the molecule concentration with a Cary 500 Scan UV–vis spectrophotometer. Calibration curve has been calculated using SBF solutions of ibuprofen in the same concentration range.

3. Results and discussion

3.1. MCM-41 prepared at mildly basic pH

Fig. 1 shows the XRD patterns of MCM-41 samples prepared at different pH from 10.8 to 9.0. Sample prepared at pH = 10.8 shows three peaks typical of the diffraction pattern of MCM-41 materials at *2 theta* values of 2.68, 4.60 and 5.10 indexed as (1 0 0), (1 1 0) and (2 0 0) reflections, respectively. The d_{100} value is 3.27 nm. The cell parameter a, calculated as $a = (2/\sqrt{3})d_{100}$, results 3.77 nm. These values are very close to those reported by Grün et al. [25]. Lowering the synthesis pH causes a loss of defined d_{110} and d_{200} peaks, and a decrease and broadening of the d_{100} peak. This is ascribed to a decrease of the mesoscopic order, since it is known that lower alkalinity usually favours the formation of disordered phases [30]. Nevertheless the presence of diffuse scattering instead of defined d_{110} and d_{200} peaks may be also due the small size of locally

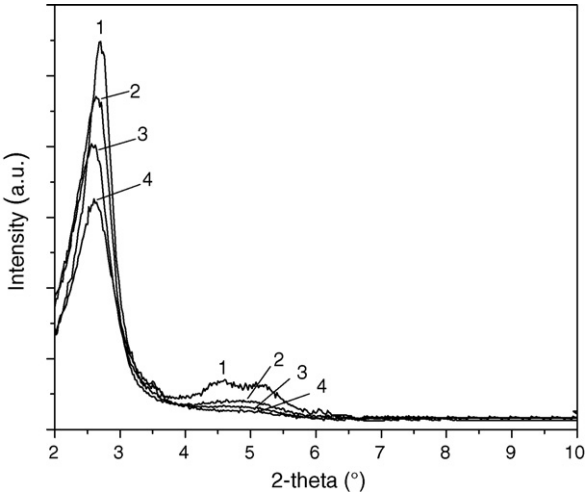

Fig. 1. XRD patterns of calcined MCM-41 samples prepared at different pH. Curve 1: MCM-41-10.8; curve 2: MCM-41-10.5; curve 3: MCM-41-9.5; curve 4: MCM-41-9.0.

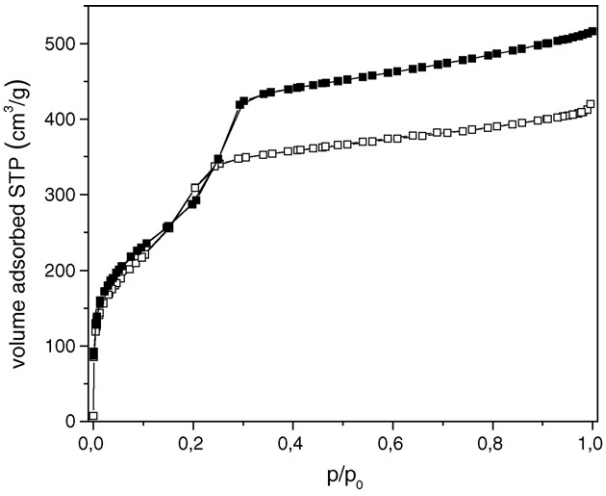

Fig. 2. Nitrogen adsorption/desorption isotherms at 77 K on MCM-41. (■) MCM-41-10.8; (□) MCM-41-9.0.

ordered domains. Upon decreasing of synthesis pH, the (1 0 0) peak shifts to lower angles, with the d_{100} values becoming equal to 3.53 for pH = 9.0. Assuming a hexagonal symmetry also for this material, the *a* parameter results 4.08.

Fig. 2 reports nitrogen adsorption/desorption isotherms for samples prepared at pH = 10.8 and 9.0. Both isotherms are of type IV, exhibiting filling of the mesopores at relative pressure p/p° below 0.3. Pore filling in MCM-41-10.8 occurs at relative pressure p/p° around 0.25, as observed by Grün et al. [25]. Values for BET specific surface area and mesopores volume are also very closed to those reported by the authors (Table 1). Pores diameter, evaluated by BJH model, results 2.4 nm. On the basis of cell parameter *a*, walls thickness results 1.32 nm. For the sample prepared at pH = 9.0, filling of mesopores occurs at lower p/p°, indicating a smaller pores size. BJH analysis gives a distribution centered at 2.0 nm. Accordingly, mesopores volume results lower, as well as BET surface area (Table 1). Mesopores filling occurs in a slightly larger range of p/p° values, in that the step in the isotherm appears less pronounced. This suggests a lower homogeneity of pores size, in agreement with a lower mesoscopic order, as evidenced by XRD results.

Considering that for the material prepared at pH = 9.0 the d_{100} value is higher and pore size is smaller, the walls thickness appears larger. This is probably due to the lower alkalinity of the synthesis batch [31].

MCM-41 materials are in form of spheres with size ranging from 200 nm to 1000 nm, similarly to what observed by Grün et al. [25] (Fig. 3a and b, at low and high magnification, respectively).

Table 1
Specific surface area (SSA), mesopore volume (V_p), pore size (D_{BJH}) and d_{100} values for MCM-41 materials

	N_2 adsorption/desorption			XRD
	SSA_{BET} (m^2/g)	V_p (cm^3/g)	D_{BJH} (nm)	d_{100} (nm)
MCM-41-10.8	1020	0.8	2.5	3.27
MCM-41-9.0	826	0.6	2.0	3.53

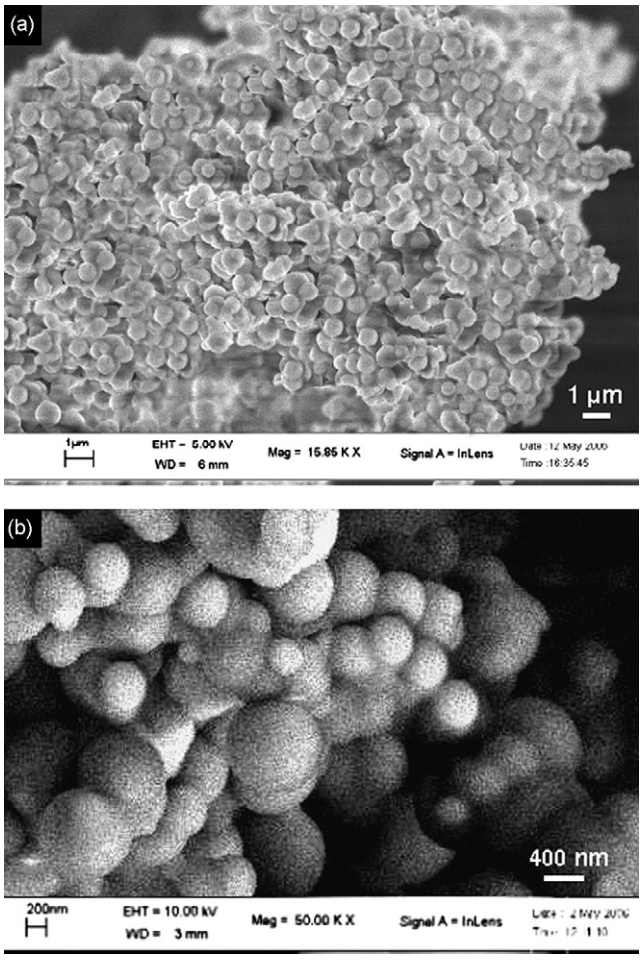

Fig. 3. SEM pictures of MCM-41-9.0 at lower (section *a*) and higher (section *b*) magnification.

All data indicate that MCM-41 prepared at pH = 9.0 maintains those properties which are interesting for drug carrier (high specific surface area, uniform porosity), ensuring a pH synthesis suitable for the maintenance of the SCK scaffold structure and properties.

3.2. MCM-41–SCK composite scaffolds

Of the four MCM-41 samples synthesized, for MCM-41–SCK composite scaffold only the sample obtained at pH = 9.0 has been considered due to its less severe synthesis conditions and thus to its lower risk of negatively affecting the scaffold integrity.

Fig. 4 shows XRD patterns of MCM-41–SCK-1 (curve 1) and MCM-41–SCK-2 (curve 2).

MCM-41–SCK-1 shows a pattern very similar to that observed for MCM-41-9.0, where only the (1 0 0) peak is observed, with a d_{100} equal to 3.42 nm. In the pattern of MCM-41–SCK-2, instead, three peaks are visible at *2 theta* values of 2.48, 4.20 and 4.78, due to (1 0 0), (1 1 0) and (2 0 0) reflections. The d_{100} is equal to 3.50 nm and the *a* parameter results 4.04.

These data suggest that, on the one hand, drying at room temperature before treatment at 90 °C is more favourable to the

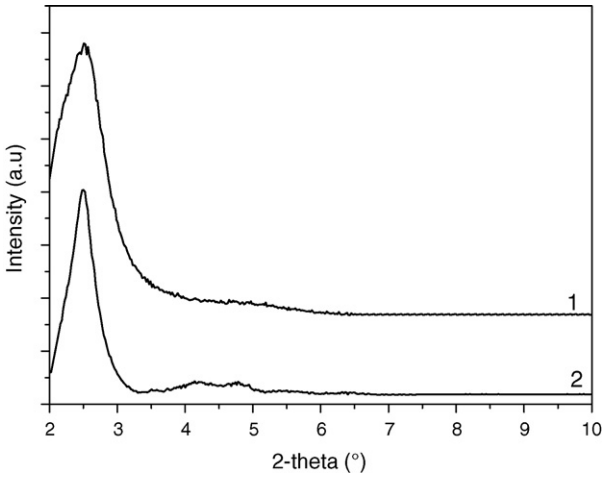

Fig. 4. XRD patterns of calcined MCM-41–SCK-1 (curve 1) and MCM-41–SCK-2 (curve 2).

formation of the mesostructure inside the scaffold. This means that a procedure resembling the powder synthesis is desirable as it concerns duration and temperature of treatments, such as drying and ageing. On the other hand, it is worth of note that the MCM-41 mesophase precipitated inside the scaffold appears more ordered than that obtained in powder form from the same synthesis solution (Fig. 1, curve 4). This may be due to a local higher pH value inside the SCK porosity, caused by a partial solubilization of basic oxides.

Fig. 5 reports nitrogen adsorption/desorption isotherms for both composites. Isotherms are of type IV and look very similar to those observed for MCM-41 powders, with pore filling occurring at relative pressure p/p° around 0.23. The difference in the scale of *y*-axis from Fig. 2 is due to the different specific weight of composites with respect to MCM-41 powders. BJH pore diameter results 2.2 nm for both systems (Table 2).

The same figure regards the adsorption/desorption isotherms of SCK-ref for comparison. No pore filling associated with mesopores is observed, as expected. A magnification shows that isotherms are of type II, typical of non-porous or macro-

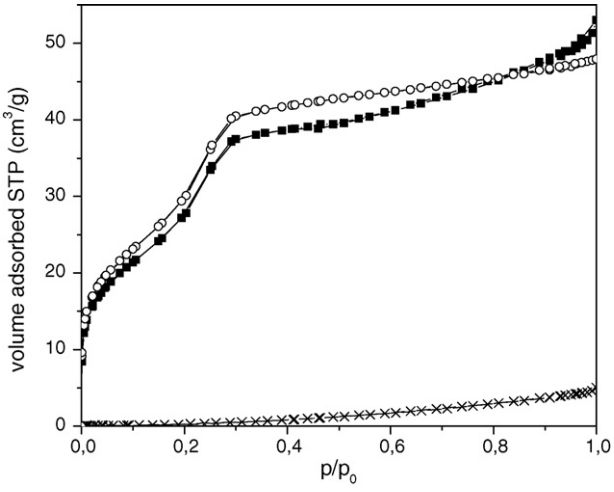

Fig. 5. Nitrogen adsorption/desorption isotherms at 77 K on MCM-41. (■) MCM-41–SCK-1; (◯) MCM-41–SCK-2; (×) SCK-ref.

Table 2
Specific surface area (SSA), mesopore volume (V_p), pore size (D_{BJH}) and d_{100} values for MCM-41–SCK systems

	SSA_{BET} (m^2/g)	V_p (cm^3/g)	D_{BJH} (nm)	d_{100} (nm)
MCM-41–SCK-1	83	0.072	2.2	3.42
MCM-41–SCK-2	107	0.084	2.2	3.50

porous adsorbent [32], with an inflection point due to complete monolayer coverage hardly distinguishable at $p/p^{\circ} < 0.02$.

SSA_{BET} calculated for MCM-41–SCK-1 and MCM-41–SCK-2 results 83 and 108 m^2/g, respectively (Table 2), i.e. some 10 times lower than that of MCM-41 powder, because most of mass sample is due to the macroporous ceramic scaffold.

An estimation of MCM-41 weight percentage in the composite scaffold may be attempted by DTG analysis, on the basis of the weight loss due to surfactant. By comparing this value with that measured for MCM-41, the amount of MCM-41 in the MCM-41–SCK composite scaffold results about 35% w/w for both the samples 1 and 2. This value is most probably overestimated, because surfactant molecules may be adsorbed or trapped also inside the scaffold pores and not only inside the mesophase.

An estimation of the MCM-41 content may be proposed also on the basis of both the SSA_{BET} values and the total volume of adsorbed nitrogen, by comparing the data measured for MCM-41, MCM-41–SCK composite scaffold and SCK-ref. This approach leads to a MCM-41 content between 10 and 15% w/w. This value, however, is uncertain because based on the assumption that the SSA_{BET} and total volume of adsorbed nitrogen are the same for the mesoporous silica in powder form and that incorporated inside the scaffold. It is probable that this latter is more sterically contrained, so that its adsorption capacity is lower: this would imply an undervaluation of the figure above.

Fig. 6 shows scanning electron micrograph of MCM-41–SCK-2 (SEM pictures related to MCM-41–SCK-1 are very similar and thus not reported), where MCM-41 spheres are clearly distinguishable from the scaffold surface, as confirmed by EDS analysis (not reported). They appear set inside the porosity of the scaffold (Fig. 6b) and on its pore walls and struts, with the same morphology and average size, also observed at high magnification (Fig. 6c). The scaffold surface is not altered by the MCM-41 synthesis as observed in Figure 6a where a quite smooth surface can be seen due to the presence of a residual amorphous phase in the glass–ceramic scaffold.

3.3. Drug uptake and release

Amounts of ibuprofen adsorbed on MCM-41-9.0, MCM-41–SCK-2 and SCK-ref from pentane solution are collected in Table 3 as weight percentage.

This was about 3.9% for SCK-ref and 11.8% for both MCM-41–SCK composite scaffolds (Table 3). The presence of mesoporous silica yields an increase of three times in the capacity of ibuprofen incorporation.

MCM-41 spheres in powder adsorbed 24.4% w/w. If the higher adsorption capacity observed for MCM-41–SCK composite scaffolds with respect to SCK-ref is ascribed entirely to

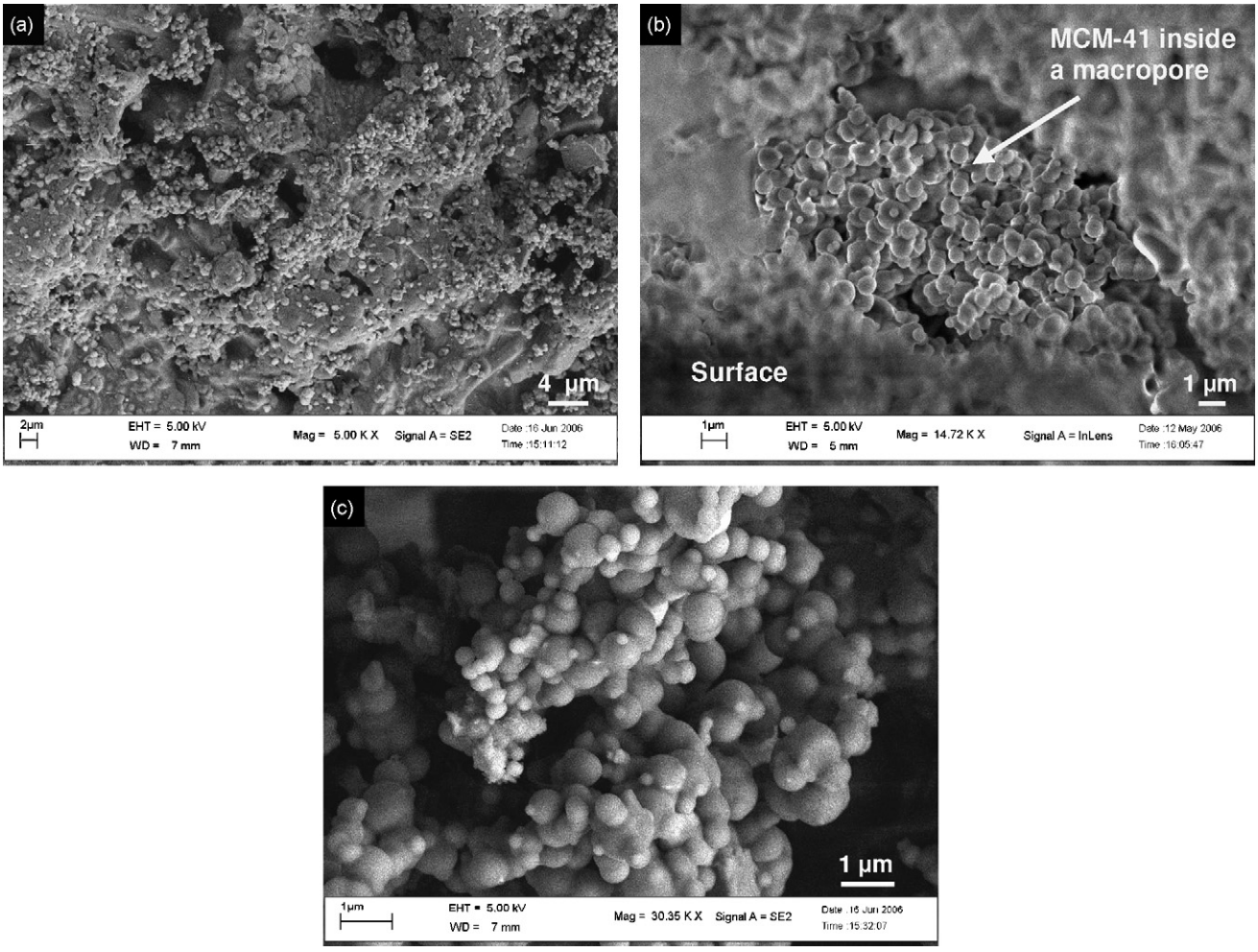

Fig. 6. SEM pictures of MCM-41–SCK-2 at lower (section *a*) and higher (sections *b* and *c*) magnification.

the presence of mesoporous silica in the former, assuming for this the same capacity measured for MCM-41 in powder, the content of mesoporous silica may be evaluated by the capacity of ibuprofen adsorption. This results 32.2% w/w in good accordance to that obtained from the DTG analysis ($\leq$35% w/w).

This value may be overestimated for similar reasons discussed above, i.e. the excess of ibuprofen molecules trapped inside MCM-41–SCK composite scaffolds with respect to SCK-ref may be not exclusively present in the silica mesophase.

Fig. 7 reports the kinetic of ibuprofen release in SBF solution from MCM-41–SCK-2 system, compared to release profiles obtained for MCM-41 in powder and SCK-ref (inset). Both MCM-41–SCK-2 and MCM-41 show two distinct regions: the former between 0 and 8 h, characterized by a very fast increase of drug concentration in SBF; the latter, between 8 and 120 h, where a slow released is observed, which seems to continue over 120 h. A step is observed between 24 and 27 h. The same feature has been observed in release curves reported in literature for

Table 3
Amount of ibuprofen up-taken by different samples upon contact with pentane solution

	Ibuprofen (wt.%)
MCM-41-9.0	24.4
SCK-ref	3.9
MCM-41–SCK-2	11.8

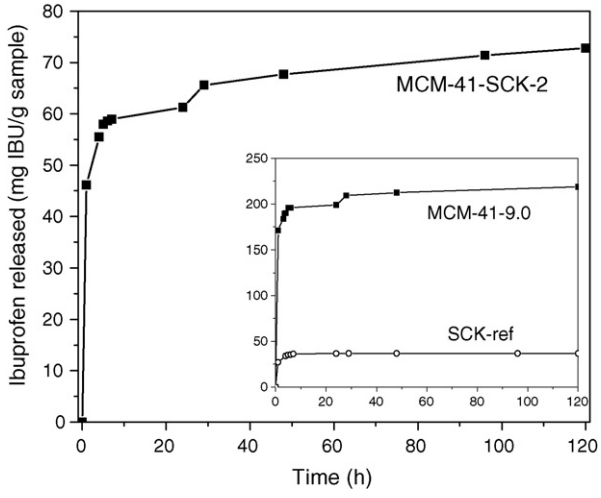

Fig. 7. Release curve in SBF at 37 °C of ibuprofen entrapped in MCM-41–SCK-2, compared with curves obtained for MCM-41-9.0 and SCK-ref (inset).

MCM-41 with similar pore size [33]. It is not observed, instead, for SBA-15–SCK composite scaffold [24]. This feature is under study on both MCM-41 and MCM-41–SCK composite scaffold.

The SCK-ref release the small amount of adsorbed ibuprofen in the first 8 h.

All data show the role of MCM-41 phase in the incorporation and release of ibuprofen from MCM-41–SCK composite scaffold.

Investigation of mechanical properties and hydroxyapatite formation on MCM-41–SCK composite scaffolds upon contact with SBF are in progress. Preliminary results show that MCM-41–SCK scaffold retains the same bioactivity of the scaffold as such and interesting mechanical properties in view of implantation, i.e. a compressive resistance value of 2.2 MPa which satisfy the requirements for a bone graft.

This suggests the feasibility of the proposed approach, i.e. the use of silica ordered mesophase incorporated inside glass–ceramic bioactive scaffolds in view of the local drug release in tissue engineering.

4. Conclusions

MCM-41 spheres have been incorporated inside the macroporosity of a bioactive glass–ceramic scaffold belonging to the SiO_2–CaO–K_2O (SCK) system.

The incorporation is achieved by impregnation of the scaffold, upon dipping, with the MCM-41 synthesis batch. The MCM-41 synthesis procedure has been modified to use somewhat lower pH values, so to minimize the scaffold degradation, in terms of bioactivity, morphology and mechanical properties, due to the impregnation procedure. The best compromise was pH = 9.0.

MCM-41–SCK composite scaffolds show peculiar features (XRD pattern, SSA_{BET}, mesopores volume and pore size) due to the presence of the ordered silica mesophase. Electron microscopy investigation reveals that MCM-41 spheres, with diameter ranging from 200 and 1000 nm, are located inside the internal macroporosity of the scaffold and on its pore walls and struts. The amount of MCM-41 incorporated was evaluated through three different methods, resulting between 10 and 35%.

The presence of MCM-41 causes a significant increase (about three times) of the ibuprofen up-take capacity of the SCK scaffold.

Ibuprofen release from MCM-41–SCK composite scaffolds in SBF occurs with kinetics very similar to that already observed by other authors for MCM-41 as such, evidencing the role of MCM-41.

As a whole, results suggest the feasibility of the use of silica ordered mesophase incorporated inside glass–ceramic bioactive scaffolds in view of the local drug release in tissue engineering.

Acknowledgements

Financial support by the Ministero Italiano della Ricerca e dell'Università (MIUR) is acknowledged (PRIN 2003, "The interface between silica-based materials and biomolecules and/or cell models". PRIN2004, "Nanostructured materials with controlled porosity for innovative technological application").

Appendix A. Supplementary data

Supplementary data associated with this article can be found, in the online version, at doi:10.1016/j.cej.2007.07.094.

References

[1] M. Vallet-Regí, Chem. Eur. J. 12 (2006) 5934.
[2] G. Balasundaram, T.J. Webster, Nanomedicine 1 (2006) 169.
[3] L.L. Hench, Curr. Opin. Solid State Mater. Sci. 2 (1997) 604.
[4] Z. Cong, W. Jianxin, F. Huaizhi, L. Bing, Z. Xingdong, J. Biomed. Mater. Res. 55 (2001) 28.
[5] H. Ramay, M. Zhang, Biomat 24 (2003) 3293.
[6] C. Vitale-Brovarone, E. Verné, L. Robiglio, P. Appendino, F. Bassi, G. Martinasso, G. Muzio, R. Canuto, Acta Biomater. 2 (2007) 199.
[7] C. Vitale-Brovarone, E. Verné, M. Bosetti, P. Appendino, M. Cannas, J. Mater. Sci.: Mater. Med. 16 (2005) 909.
[8] L.L. Hench, J. Am. Ceram. Soc. 74 (1991) 1487.
[9] M. Rucker, M.W. Laschke, D. Junker, C. Carvalho, A. Schramm, R. Mulhaupt, N.C. Gellrich, M.D. Menger, Biomaterials 27 (2006) 5027.
[10] P. Collin-Osdoby, L. Rothe, S. Bekker, F. Anderson, Y.F. Huang, P. Osdoby, J. Bone Min. Res. 17 (2002) 1859.
[11] A. Rösler, G.W.M. Vandermuelen, H.A. Klok, Adv. Drug Deliv. Rev. 53 (2001) 95.
[12] J.D. Badjiæ, N.M. Kostiæ, J. Phys. Chem. B 104 (2000) 11081.
[13] E.M. Santos, S. Radin, P. Ducheyne, Biomaterials 20 (1999) 1695.
[14] H. Goto, T. Isobe, M. Senna, J. Nanopart. Res. 1 (1999) 205.
[15] M. Vallet-Regí, A. Rámila, R.P. del Real, J. Pérez-Pariente, Chem. Mater. 13 (2001) 308.
[16] C.T. Kresge, M.E. Leonowicz, W.J. Roth, J.C. Vartuli, J.S. Beck, Nature 359 (1992) 710.
[17] J. Andersson, J. Rosenholm, S. Areva, M. Lindén, Chem. Mat. 16 (2004) 4160.
[18] G. Cavallaro, P. Pierro, F.S. Palumbo, F. Testa, L. Pasqua, R. Aiello, Drug Deliv. 11 (2004) 41.
[19] R. Aiello, G. Cavallaro, G. Giammona, L. Pasqua, P. Pierro, F. Testa, Stud. Surf. Sci. Catal. 142 (2002) 1165.
[20] C. Tourné-Péteilh, D. Brunel, S. Bégu, B. Chiche, F. Fajula, D.A. Lerner, J.M. Devoisselle, New J. Chem. 27 (2003) 1415.
[21] B. Fubini, in: A.P. Legrand (Ed.), The Surface Properties of Silicas, vol. 414, York, John Wiley & Sons, New York, 1998, Chap. 5.
[22] B. Onida, V. Cauda, S. Fiorilli, E. Vernè, C. Vitale Brovarone, D. Viterbo, G. Croce, M. Milanesio, E. Garrone, Stud. Surf. Sci. Catal. 158b (2005) 2027.
[23] C. Vitale Brovarone, E. Verné, P. Appendino, J. Mater. Sci. Mat. Med. 17 (2006) 1069.
[24] V. Cauda, S. Fiorilli, B. Onida, E. Vernè, C. Vitale Brovarone, D. Viterbo, G. Croce, M. Milanesio, E. Garrone, J. Mater. Chem., in press.
[25] M. Grün, K.K. Unger, A. Matsumoto, K. Tsutsumi, Microp. Mesop. Mater. 27 (1999) 207.
[26] E.P. Barrett, L.G. Joyner, P.P. Halenda, J. Am. Chem. Soc. 73 (1951) 373.
[27] C. Armstrong, Arch. Clin. Neuropsychol. 10 (1995) 1.
[28] J.G.M. van Engelen, W. Rebel-de Haan, J.J.G. Opdam e, G.J. Mulder, Toxicol. Appl. Pharmacol. 144 (1997) 385.
[29] T. Kokubo, H. Kushitani, S. Sakka, T. Kisugi, T. Yamamuro, J. Biomed. Mater. Res. 24 (1990) 721.

[30] F. Di Renzo, A. Galarneau, P. Trens, F. Fajula, in: F. Schüth, K. Sing, J. Weitkamp (Eds.), Handbook of Porous Materials, Wiley-VCH, 2002, p. 1311.
[31] F. Di Renzo, F. Testa, J.D. Chen, H. Cambon, A. Galarneau, D. Plee, F. Fajula, Microp. Mesop. Mater. 28 (1999) 437.
[32] S. Lowell, J.E. Shields, M.A. Thomas, M. Thommes, Characterization of porous solids and powders: surface area, pore size and density, Kluwer Academic Publishers, Dordrecht, 2004.
[33] P. Horcajada, A. Rámila, J. Pérez-Pariente, M. Vallet-Regí, Microp. Mesop. Mater. 68 (2004) 105.